Real-time analysis of the optical response of cavity bipolaritons: Four-wave mixing and dynamics of formation

Hisaki Oka and Hajime Ishihara
Department of Physics and Electronics, Osaka Prefecture University, 1-1 Gakuen-cho, Naka-ku, Sakai 599-8531, Japan
(Received 18 April 2008; revised manuscript received 18 August 2008; published 14 November 2008)

We theoretically investigate the four-wave mixing (FWM) of a biexciton in a microcavity in the framework of cavity bipolariton. Cavity bipolaritons are stably formed in the strong-coupling regime with an exciton-cavity coupling comparable to the biexciton binding energy. The FWM signal obtained from our bipolariton model, where the biexciton and unbound two-exciton states form a complete system, agrees well with the experimental data [Baars *et al.*, Phys. Rev. B **63**, 165311 (2001)]. A strong FWM signal is obtained when a cavity bipolariton is formed by a superposition state of a biexciton and unbound two-cavity-polariton states. We also analyze the dynamics of the formation of biexciton and cavity polaritons by numerically solving the optical master equation in time domain. Efficient excitation of cavity bipolariton requires a specific pulse duration and/or pulse delay so that two-cavity polaritons are formed before the biexciton is excited.

DOI: 10.1103/PhysRevB.78.195314 PACS number(s): 78.67.−n, 71.36.+c, 42.50.Md

I. INTRODUCTION

Strong optical nonlinearities of excitons confined in a semiconductor microcavity have attracted much attention because of their potential applications to quantum information and communication technologies.[1,2] The optical properties of cavity polaritons, formed by strongly coupling excitons with a cavity field, have been extensively investigated, and now increasing attention has been paid to optical nonlinearities due to the formation of biexciton in a microcavity. In particular, the recent observation of entangled photons from biexcitons in a bulk semiconductor[3] and the development of semiconductor microcavities trigger researches toward the development of integrated and highly efficient entangled-photon devices by lower-dimensional semiconductors.[4–7] In such devices, the realization of efficient biexciton-cavity coupling is a key issue.

When excitons are confined in a microcavity, they are subject to two types of interactions. One is the exciton-photon interaction leading to the cavity polaritons, characterized by the exciton-cavity coupling $\hbar g$. Another is the exciton-exciton interaction leading to biexciton formation, characterized by the biexciton binding energy Δ_B. As a result of these interactions, an exciton-cavity system forms a new eigenstate of a bound two-cavity-polariton state (called a cavity bipolariton). An important consideration is then that the cavity bipolaritons are stable only for $\hbar g \sim \Delta_B$. As discussed by Baars *et al.*,[8] the resulting optical response in this condition can be understood in the bipolariton framework unlike for the limiting cases, $\hbar g \ll \Delta_B$ or $\hbar g \gg \Delta_B$, where cavity bipolaritons are not sufficiently stable.[9,10]

In the analysis in Ref. 8, however, they take no account of unbound two-exciton states and the internal degrees of freedom of biexciton, corresponding to the relative motions of the two constituent excitons of biexciton. In previous work,[7] we have clarified that unbound two-cavity-polariton states formed by unbound two-exciton states play an important role in cavity-bipolariton formation, and this can be understood only by properly treating complete center-of-mass (c.m.) degrees of freedom of the two-exciton states. We therefore introduce a general model containing both a biexciton and unbound two-exciton states, which form a complete system, and theoretically analyze the four-wave mixing (FWM) of cavity bipolaritons. We show that a strong FWM signal can be obtained when a cavity bipolariton is formed by a superposition state of biexciton and unbound two-cavity-polariton states. The cavity bipolariton formed in this way optimizes the nonlinearity of a biexciton coupled with cavity fields, and we have demonstrated that highly efficient generation of entangled photons can then be realized.[7] We also analyze the dynamic formation of cavity bipolaritons by numerically solving the optical master equation describing the biexciton-cavity coupling in time domain. We show that there is a specific pulse duration and/or pulse delay for efficient excitation of cavity bipolaritons.

The rest of this paper is organized as follows. In Sec. II, we formulate an exciton-cavity system, forming a complete set of bound and unbound two-exciton states, and the optical master equation in the framework of cavity bipolariton. In Sec. III, we numerically analyze the FWM and the dynamics of the formation of cavity bipolaritons. In Sec. IV, we summarize our results.

II. THEORETICAL MODEL

We consider a quantum well (QW) embedded in a distributed Bragg reflector microcavity (DBR cavity) as depicted in Fig. 1(a), where a $\lambda/2$ DBR cavity with a cavity length of L is assumed and the QW is placed at the antinode of the cavity mode. Two pulses are normally incident on the surface of the DBR cavity, so that the cavity bipolaritons with an in-plane c.m. momentum of zero are excited. In this work, we focus on the FWM signal emitted in the incident direction by using the input-output theory. For simplicity, in these optical processes, we ignore spontaneous emission of exciton into non-cavity modes, nonradiative decay of exciton, and a biexciton decay to interface modes of cavity fields.[11]

The Hamiltonian for the fundamental mode of a $\lambda/2$ DBR cavity field is given by

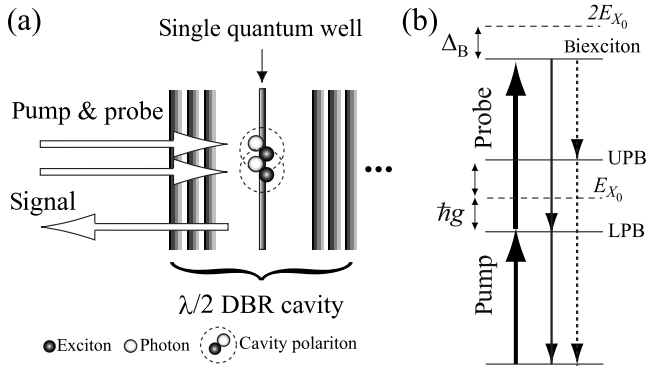

FIG. 1. Schematics of (a) the cavity-QW system and (b) the optical excitation of a cavity bipolariton. The pump energy is tuned to the LPB and the probe energy is tuned to the energy difference between the biexciton and LPB.

$$\hat{H}_C = \hbar \sum_k \omega_k \hat{c}_k^\dagger \hat{c}_k, \quad \text{with} \quad \omega_k = \omega_0 \sqrt{1 + (kL/\pi)^2}, \tag{1}$$

where $\hat{c}_k(\hat{c}_k^\dagger)$ is the annihilation (creation) operator of the cavity photon with an in-plane wave vector k and ω_k is the dispersion of the cavity photon. Using an exciton annihilation (creation) operator $\hat{b}_k(\hat{b}_k^\dagger)$, the interaction Hamiltonian describing the exciton-cavity coupling can be written as

$$\hat{H}_{\text{int}} = \hbar \sum_k g_k (\hat{c}_k^\dagger \hat{b}_k + \hat{c}_k \hat{b}_k^\dagger), \tag{2}$$

where g_k is the exciton-cavity coupling rate or the Rabi frequency. When the exciton-cavity coupling rate is larger than the spontaneous emission rate of exciton and the cavity damping rate, excitons are strongly coupled to cavity photons, forming a new eigenstate called a cavity polariton.

The exciton Hamiltonian in the semiconductor model is usually described as $\hat{H}_X = \int dk \hbar \omega_{X_k} \hat{b}_k^\dagger \hat{b}_k + \hat{V}_C$, where $\hat{V}_C$ is the exciton-exciton interaction with an appropriate spin combination. Furthermore, the exciton dispersion ω_{X_k} is often assumed to be parabolic using the effective-mass approximation. This kind of exciton model is useful for small k but complicated to discuss the biexciton formation owing to continuum model. In this work, we adopt a discrete lattice exciton model because it provides tractable solutions of bound and unbound two-exciton states as a complete set. This approach is reasonable for grasping the essential mechanism arising from the degrees of freedom of in-plane c.m. motions especially the cavity-bipolariton formation. For simplicity, we ignore the spin degree of freedom[12] and restrict free propagation of the excitons to one direction parallel to the surface of the DBR cavity. Assuming a one-dimensional periodic lattice, the Hamiltonian of the exciton system can then be described as

$$\hat{H}_X = \epsilon \sum_\ell \hat{b}_\ell^\dagger \hat{b}_\ell - t \sum_\ell (\hat{b}_{\ell+1}^\dagger \hat{b}_\ell + \hat{b}_\ell^\dagger \hat{b}_{\ell+1}) + V \sum_\ell \hat{b}_\ell^\dagger \hat{b}_\ell^\dagger \hat{b}_\ell \hat{b}_\ell + \Delta \sum_\ell \hat{b}_\ell^\dagger \hat{b}_{\ell+1}^\dagger \hat{b}_{\ell+1} \hat{b}_\ell, \tag{3}$$

where $b_\ell(b_\ell^\dagger)$ is the exciton annihilation (creation) operator at the ℓth site, ϵ is the excitation energy of each site, and t is the transfer energy of exciton from a site to neighboring sites. Interactions between two excitons are described by the last two terms. The third term prohibits two excitons from occupying the same site ($V \to \infty$), corresponding to the Pauli exclusion principle, and the last term is the attractive interaction between two neighboring excitons ($\Delta < 0$), leading to biexciton formation. The eigenenergy and eigenstate for a one-exciton state are respectively given by

$$E_{X_k} = \epsilon - 2t \cos ka \quad \text{and} \quad |X_k\rangle = \frac{1}{\sqrt{N}} \sum_\ell e^{ik\ell a} \hat{b}_\ell^\dagger |0\rangle, \tag{4}$$

where a is the lattice constant and N is the lattice period. Eigenstates for two-exciton states with zero c.m. momentum can be described using direct products of one-exciton eigenstates with opposite k, $|X_k X_{-k}\rangle \equiv |X_k\rangle \otimes |X_{-k}\rangle$, as

$$|B\rangle = \sum_k C_k^B |X_k X_{-k}\rangle \quad \text{and} \quad |S_\mu\rangle = \sum_k C_k^\mu |X_k X_{-k}\rangle, \tag{5}$$

where $|B\rangle$ is the biexciton state and $\{|S_\mu\rangle\}_\mu$ are the unbound two-exciton states. The expansion coefficients C_k are numerically calculated and determined so that $|B\rangle$ and $\{|S_\mu\rangle\}_\mu$ form a complete system. Concretely, we consider the two-exciton state with site representation, $|\mu\rangle = \Sigma_{\ell<m} C_{\ell,m}^\mu |\ell, m\rangle$, where $|\ell, m\rangle \equiv |\ell\rangle \otimes |m\rangle$. Note that $|m, m\rangle$ for any m are excluded in the expansion. This prohibition of two excitons occupying the same site corresponds to $V \to \infty$. We numerically calculate $C_{\ell,m}^\mu$ and obtain the k representation of $|\mu\rangle$ by Fourier transforming $C_{\ell,m}^\mu$ to $C_{k,k'}^\mu$. A similar calculation method of C_k is found in Ref. 13. The biexciton binding energy Δ_B is uniquely determined by t and Δ[14] and converges for $N \to \infty$.

The eigenstates of the cavity-QW system can now be obtained by diagonalizing the Hamiltonian $\hat{H}_{\text{sys}} = \hat{H}_X + \hat{H}_C + \hat{H}_{\text{int}}$. Rewriting the exciton operator $\hat{b}_k$ in Eq. (2) with the Hubbard operators as[15]

$$\hat{b}_k = |G\rangle\langle X_k| + \sum_{k'} \langle X_{k'}|\hat{b}_k|X_k X_{k'}\rangle |X_{k'}\rangle\langle X_k X_{k'}|, \tag{6}$$

the eigenstates can be expressed, in form, as

$$|1p\rangle^\pm = \alpha_x |X;0\rangle \pm \alpha_c |G;1\rangle, \tag{7}$$

$$|2p\rangle = \alpha_{xx} |XX;0\rangle + \alpha_{xc} |X;1\rangle + \alpha_{cc} |G;2\rangle, \tag{8}$$

where $|G\rangle$ is the ground state and the separation by a semicolon denotes $|\text{exciton};\text{photon}\rangle$. $|1p\rangle^-$ is lower cavity-polariton branch (LPB) and $|1p\rangle^+$ is upper cavity-polariton branch (UPB). $|2p\rangle$ is the two-cavity-polariton state consisting of the two-exciton state $|XX;0\rangle$, the one-exciton-one-photon state $|X;1\rangle$, and the two-photon state $|G;2\rangle$. In particular, when $|2p\rangle$ is near a bare biexciton energy level, a cavity bipolariton is formed. In this study, we consider the coherent regime of biexciton excitation (weak excitation)

and thus only the cavity-polariton states up to $|2p\rangle$ are needed.[16] The biexciton-cavity coupling can be described as

$$\hbar g_k^B = \langle X_{-k}; 1_k | \hat{H}_{\text{int}} | B; 0 \rangle = \hbar g_k C_k^B \langle X_{-k} | \hat{b}_k | X_k X_{-k} \rangle. \quad (9)$$

Equation (9) means that $|B\rangle$ can be coupled with cavity fields with various k through the expansion bases $\{|X_k X_{-k}\rangle\}$. $\hbar g_k^B$ can, in principle, be uniquely determined by g_k and C_k^B. However, the value of transition dipole moment in g_k is modified from the actual value owing to simplification of our model. Therefore, to compensate it, we introduce a variable of ζ as $\zeta \hbar g_k^B \rightarrow \hbar g_k^B$ and determine ζ by fitting to the experimental data of Ref. 8, where k dependence of ζ is ignored for simplicity because the exciton dispersion is almost negligible as compared to the cavity dispersion.

The FWM signal from the cavity-QW system can be analyzed using the optical master equation and input-output theory.[17] When spontaneous emission of excitons into noncavity modes is ignored, the master equation is given by

$$\frac{d}{dt}\hat{\rho} = \frac{1}{i\hbar}[\hat{H}_{\text{sys}} + \hat{H}_{\text{ext}}, \hat{\rho}] + \sum_k \kappa (2\hat{c}_k^\dagger \hat{\rho} \hat{c}_k - \hat{c}_k^\dagger \hat{c}_k \hat{\rho} - \hat{\rho} \hat{c}_k^\dagger \hat{c}_k), \quad (10)$$

where κ is the cavity damping rate and $\hat{H}_{\text{ext}}$ is the interaction Hamiltonian between intracavity photons and linearly polarized classical input lights, $\xi_{\text{pump}}(t)$ and $\xi_{\text{probe}}(t)$, given by

$$\hat{H}_{\text{ext}} = i\hbar\sqrt{2\kappa}\hat{c}_0[\xi_{\text{pump}}(t) + \xi_{\text{probe}}(t)] + \text{H.c.} \quad (11)$$

For the excitation of $|2p\rangle$, we use the resonant excitation condition where the energy of the pump beam is tuned to the LPB ($\hbar\omega_{\text{pump}} = E_{\text{LPB}}$) and that of the probe beam is tuned to the energy difference between the biexciton and the LPB ($\hbar\omega_{\text{probe}} = E_B - E_{\text{LPB}}$), so that the biexciton component in $|2p\rangle$ can be resonantly excited [see Fig. 1(b)]. Throughout this work, we use the resonant excitation condition with zero time delay between pump and probe beams. According to the input-output theory,[17] the output photon with $k=0$ can be described as

$$\xi_{\text{output, } k=0}(t) = \xi_{\text{input, } k=0}(t) + \sqrt{2\kappa}\,\text{Tr}[c_0\hat{\rho}(t)]. \quad (12)$$

Equation (12) means that the output is given by a superposition of the input photon reflected by the cavity and the photon emitted through the cavity mode of $k=0$, corresponding to the FWM signal. We separate the FWM signal from the incident photons by considering only the last term in Eq. (12). The density matrix $\rho(t)$ of cavity-QW system can be obtained by numerically solving the master equation, e.g., using the Runge-Kutta method, and the FWM spectra are obtained by Fourier transforming Eq. (12).

III. RESULTS

In this section, we numerically analyze the FWM signal of cavity bipolaritons. First, we calculate the eigenenergies of cavity bipolaritons and evaluate the biexciton-cavity coupling by fitting to the experimental data in Ref. 8. Second, we analyze in detail the nondegenerate FWM signal of cavity bipolaritons and show that a strong FWM signal can be obtained when a cavity bipolariton formed by a superposition state of a biexciton and unbound two-cavity-polariton states is realized. Finally, we discuss the dynamics of the formation of biexciton and cavity polaritons in terms of the dependence on incident pulse duration.

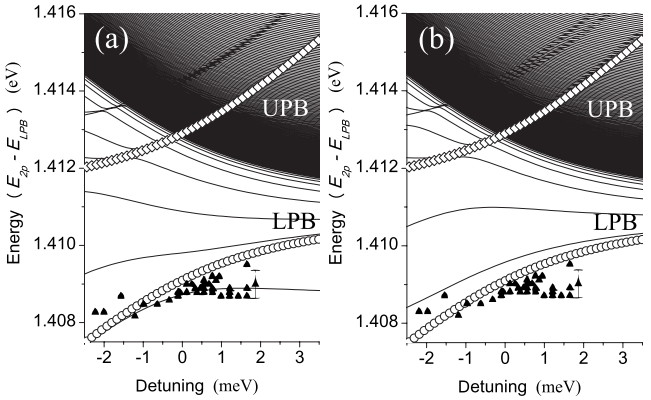

FIG. 2. Energies of $|2p\rangle$ as a function of $\Delta\omega$ for (a) $\hbar g_0^B = 0.7$ meV and (b) $\hbar g_0^B = 1.75$ meV. The calculation parameters are $\Delta_B = 2.2$ meV, $\hbar g_0 = 1.9$ meV, and $N = 10001$. The open symbols ◯ and ♢ correspond to the signal peaks from the LPB to the ground state and from the UPB to the ground state, respectively. The full symbols are the bipolariton peaks measured in the experiment of Ref. 8.

Figure 2 shows the eigenenergies of $|2p\rangle$, E_{2p} as a function of detuning $\Delta\omega = (\hbar\omega_0 - E_{X_0})$ for two different biexciton-cavity couplings: (a) $\hbar g_0^B = 0.7$ meV and (b) $\hbar g_0^B = 1.75$ meV. The vertical axes are $E_{2p} - E_{\text{LPB}}$, corresponding to the signal energy emitted from $|2p\rangle$ to the LPB. From the calculation of transition amplitudes, we obtain $|\langle \text{LPB}|\hat{c}_0|2p\rangle|^2 \gg |\langle \text{UPB}|\hat{c}_0|2p\rangle|^2$ and can therefore ignore the emission from $|2p\rangle$ to the UPB. The open symbols correspond to peaks of the emission from the LPB to the ground state and from the UPB to the ground state. To compare to the experimental result (full symbols), the exciton energy is set to $E_{X_0} = 1.411$ eV, biexciton binding energy is $\Delta_B = 2.2$ meV, and the exciton-cavity coupling is $\hbar g_0 = 1.9$ meV. For $\hbar g_0^B = 0.7$ meV, we obtain good agreement between the experimental data and the theoretical results near ≈ 1.409 eV,[18] as can be seen in Fig. 2(a). Baars *et al.*[9] have estimated $\hbar g_{k\approx 0}^B \approx 1.75$ meV, comparable to $\hbar g_0$, by introducing a similar bipolariton model. However their result might be an overestimate because they take no account of the degrees of freedom of relative motions of biexciton. A biexciton has relative momenta even though its c.m. momentum is zero so that the biexciton can be coupled with cavity photons of various k, as shown in Eq. (9). As a result, the biexciton-cavity coupling to a cavity field k becomes effectively small. For comparison, our results for $\hbar g_0^B = 1.75$ meV are shown in Fig. 2(b). The energy level found near ≈ 1.409 eV in Fig. 2(a) moves to far lower energy and cannot be found in Fig. 2(b). Thus, the exciton model forming a complete set of two-exciton states in k space, as presented in this work, is required for the more detailed analysis of biexciton-cavity coupling and cavity-bipolariton formation.

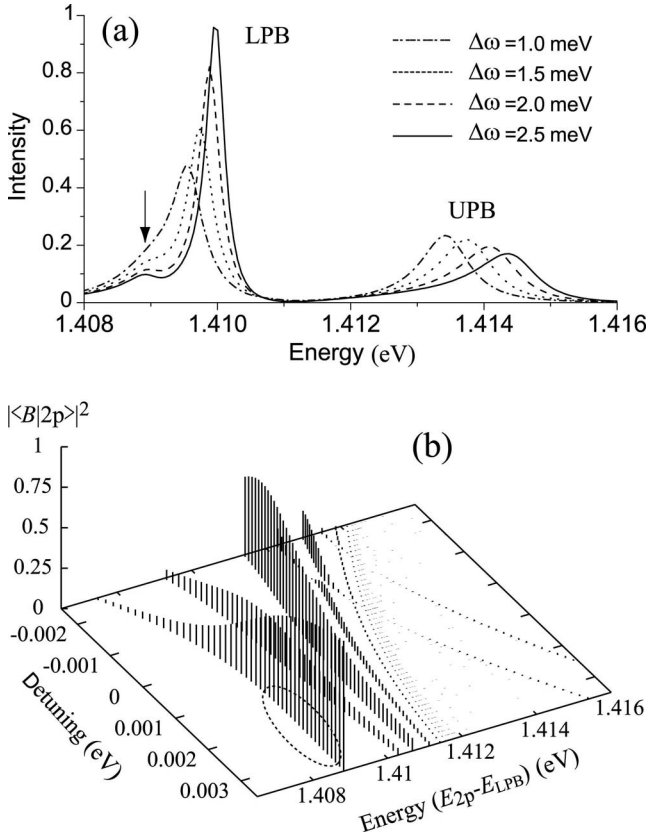

FIG. 3. (a) FWM spectra for $\Delta\omega=1.0, 1.5, 2.0$, and 2.5 meV, where $2\hbar\kappa=1.41$ meV, $\sigma=200$ fs, and the other parameters are the same as those in Fig. 2(b). (b) Probability amplitudes of the biexciton component $|\langle B|2p\rangle|^2$.

Figure 3(a) shows the FWM signal for $\Delta\omega=1.0$, 1.5, 2.0, and 2.5 meV. The cavity damping is set to $2\hbar\kappa=1.41$ meV, corresponding to a quality factor of $Q=1000$, and the other parameters of the cavity-QW system are the same as those in Fig. 2(a). The pump and probe beams are Gaussian pulses with a pulse width of $\sigma=200$ fs and an intensity of $\sim 7.5 \times 10^9$ cm^{-2}. The dominant FWM peaks are the signals from the LPB at ≈ 1.410 eV and from the UPB at ≈ 1.414 eV. Below the LPB signal, however, an additional peak can be clearly seen at the energy slightly below ≈ 1.409 meV (indicated by arrow).[19] This additional peak, dependent on $\Delta\omega$, arises from a biexciton component in $|2p\rangle$, as can be seen from the amplitude probability $|\langle B|2p\rangle|^2$ in Fig. 3(b). As $\Delta\omega$ increases, the biexciton component at ≈ 1.409 eV gradually increases and dominates $|2p\rangle$ for $\Delta\omega \gtrsim 1.5$ meV (indicated by dotted circle). In other words, however, this means that the cavity-photon components in $|2p\rangle$ decrease. As a result, for the increase of $\Delta\omega$, the peak shape sharpens owing to increase in biexciton component, but the peak intensity weakens owing to decrease in cavity-photon components.[20] This tradeoff between the biexciton and the cavity photons always arises in the formation of cavity bipolariton. Therefore, careful control of cavity-QW parameters is required in order to obtain a strong FWM signal of the cavity bipolariton so that both the biexciton excitation by input photons and the photon emission through an output cavity field can be efficiently realized.

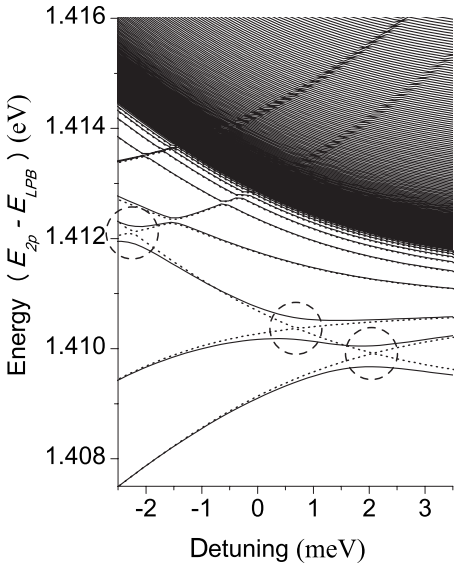

FIG. 4. Energies of $|2p\rangle$ for $\hbar g_0^B=0.24$ meV. The other calculation parameters are the same as those in Fig. 2(a). Cavity bipolaritons with level anticrossing are indicated by dashed circles. The dotted lines are a bare biexciton and noninteracting cavity polaritons ($\hbar g^B=0$).

In previous work, we have clarified that such a cavity-bipolariton state can be simply and efficiently obtained by realizing a level anticrossing of a bare biexciton and two-cavity polaritons formed by unbound two-exciton states.[7] The cavity bipolariton with the level anticrossing is obtained at a bare biexciton energy level and can be described, in form, as

$$|2p\rangle \approx |B\rangle \pm (|S;0\rangle + |X_{\pm k};1_{\mp k}\rangle + |G;1_{\pm k}1_{\mp k}\rangle). \quad (13)$$

This means that the biexciton remains almost bare and is weakly coupled with cavity photons through unbound two-cavity-polariton states. The level anticrossing is achieved only when the exciton-cavity coupling $\hbar g$ is comparable to the biexciton binding energy Δ_B. The splitting width of the anticrossing then corresponds to $2\hbar g_0^B$. To clearly show the behavior of the level anticrossing, we plot E_{2p} for small value of $\hbar g_0^B$ in Fig. 4. The level anticrossings occur at the points where unbound two-cavity-polariton states intersect with a bare biexciton (indicated by dashed circles).[21] In particular, the cavity bipolariton for $k \approx 0$ is at ≈ 1.4095 eV for $\Delta\omega=2.0$ meV, and in the Baars experiment they realized this level anticrossing by utilizing cavity detuning. A strong FWM signal can thus be obtained from a cavity bipolariton with a level anticrossing. In general, level anticrossing points vary with the value of $\hbar g$ and with desired output mode k. Therefore, it would be difficult to observe a cavity-bipolariton signal without an appropriately designed cavity-QW system.

Finally, we investigate the dynamics of cavity-bipolariton formation in terms of the dependence on σ. Figure 5 shows the dynamics of the population components of $|1p\rangle$ [(a)–(c)] and $|2p\rangle$ [(d)–(f)] and the FWM spectra [(g)–(i)] for pulse durations of $\sigma=50$, 250, and 1000 fs. The parameters of cavity-QW system are the same as those in Fig. 2(a) and the

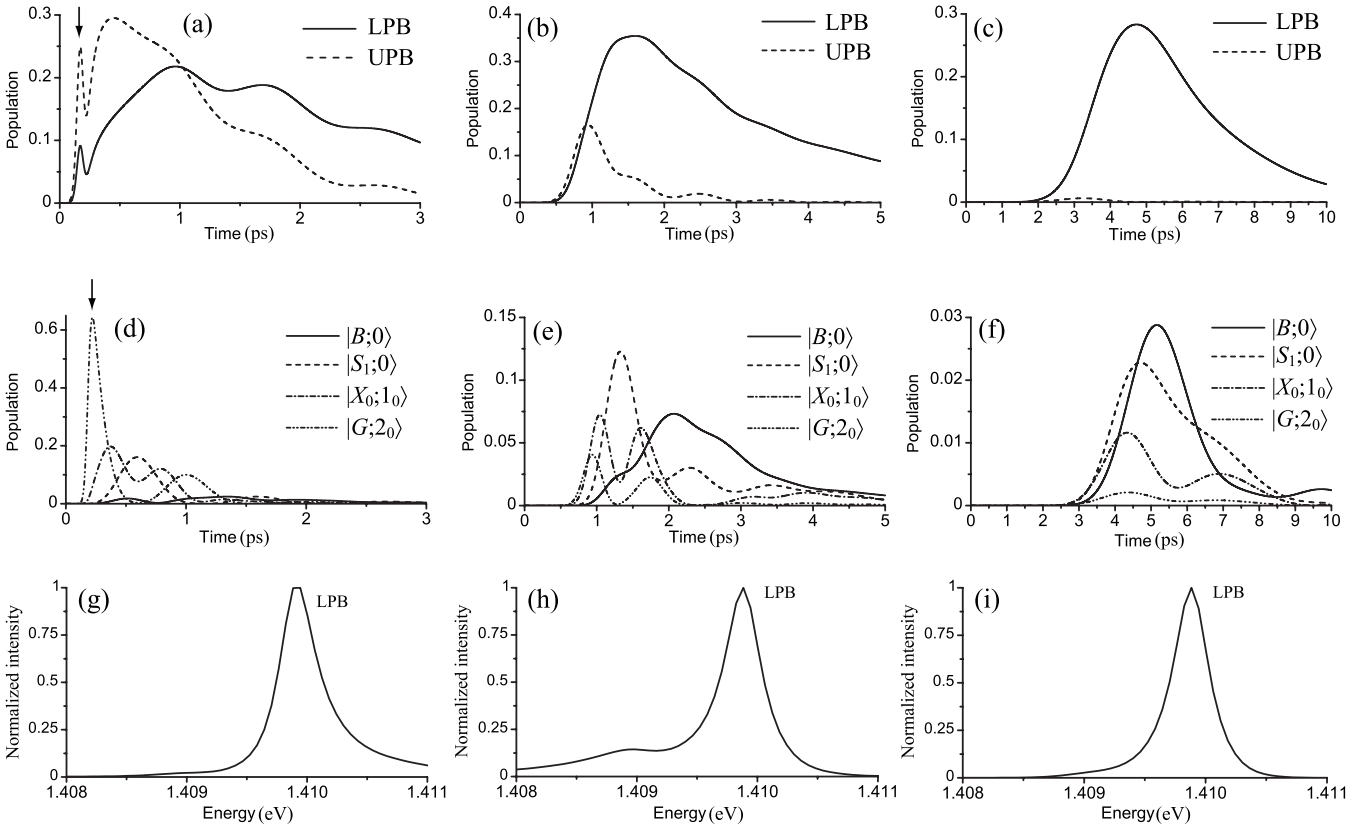

FIG. 5. Dynamics of the population components of (a)–(c) $|1p\rangle$ and (d)–(f) $|2p\rangle$ for incident pulses with three different σ. (a) and (d) are for $\sigma=50$ fs, (b) and (e) for $\sigma=250$ fs, and (c) and (f) for $\sigma=1000$ fs. (g)–(i) are the FWM signals for $\sigma=50$, 250, and 1000 fs, respectively. $|S_1\rangle$ is the unbound two-exciton state having the lowest energy. The calculation parameters are $\Delta_B=2.2$ meV, $\hbar g_0=1.9$ meV, $\hbar g_0^B=0.7$ meV, and $\Delta\omega=2.0$ meV.

resonant excitation condition is used. The power of incident light is varied to keep the intracavity mean-photon numbers effectively the same for each σ, and the signal intensity is normalized by its peak value. When σ is shorter than ≈ 1 ps, corresponding to the Rabi splitting $2\hbar g$, the LPB and UPB are simultaneously excited by the first incident photon, but the photonlike UPB increases first followed by the excitonlike LPB, as can be seen in Figs. 5(a) and 5(b). The beat with a period of ≈ 1 ps, observed when the LPB and UPB grow enough, is the quantum beat between the LPB and UPB. For the short pulse with $\sigma=50$ fs [(a) and (d)], a subsequent incident photon immediately and strongly excites $|G;2_0\rangle$ before the LPB and UPB grow enough so that $|G;2_0\rangle$ dominates $|2p\rangle$ (indicated by arrows). This leads to strong suppression of biexciton formation, and therefore the bipolariton signal is hardly observed [Fig. 5(g)]. For the increase of σ to $\sigma=250$ fs [(b) and (e)], the immediate excitation to $|G;2_0\rangle$ is suppressed, owing to the low excitation of the photonlike UPB. In this case, $|X_0;1_0\rangle$ becomes comparable to $|G;2_0\rangle$ and $|B;0\rangle$ is efficiently formed through $|X_0;1_0\rangle$, with time delay of ~ 1 ps. As a result, a strong FWM signal of cavity bipolariton can be observed at ≈ 1.409 eV [Fig. 5(h)]. For further increase of σ to $\sigma=1000$ fs, comparable to the Rabi splitting, the excitation of the UPB is strongly suppressed and the excitonlike LPB dominates $|1p\rangle$. Although the population of $|B;0\rangle$ is then highest in $|2p\rangle$ [see Fig. 5(f)], the bipolariton signal is hardly observed in Fig. 5(i) because the photon component in $|2p\rangle$ is low. In particular, for the limiting case of continuous-wave excitation (i.e., $\sigma\rightarrow\infty$), the FWM signal of cavity bipolariton cannot be observed at all. These results mean that there is a specific value of σ at which the cavity bipolariton is most efficiently excited. The specific σ would be different by the cavity-QW parameters, especially C^B.

In the dynamic formation of cavity bipolaritons, there is thus a tradeoff between biexciton and photon components, similar to the tradeoff between the signal shape and peak intensity discussed in Fig. 3. Simultaneous excitation of $|X;1\rangle$ and $|G;2\rangle$ before $|B;0\rangle$ then plays a key role in obtaining a strong FWM signal. Efficient excitation of cavity bipolariton is therefore summarized as follows: (i) Excite both $|X;0\rangle$ and $|G;1\rangle$ by the first incident photon, then (ii) induce $|X;1\rangle$ and $|G;2\rangle$ by the second incident photon through $|X;0\rangle$ and $|G;1\rangle$, and finally (iii) $|B;0\rangle$ is excited through $|X;1\rangle$ with a time delay corresponding to the Rabi oscillation. For the present parameters, condition (i) corresponds to the simultaneous excitation of the LPB and UPB by pulses with σ shorter than the Rabi oscillation. The point in condition (ii) is to suppress the immediate excitation to $|G;2\rangle$ by a subsequent input photon with a time delay of ≈ 1 ps, corresponding to the Rabi splitting $2\hbar g$, so that the LPB and UPB can grow enough. This kind of delay excitation can also be realized simply by using two time-delayed pulses, even for short pulses, as often used in the FWM analyses.

IV. CONCLUSIONS AND DISCUSSION

We have theoretically investigated the FWM of cavity bipolaritons by introducing an exciton model forming a complete set of bound and unbound two-exciton states. The FWM signal obtained from the bipolariton model presented in this work could well explain the experimental data in Ref. 8. We have shown that in the cavity-bipolariton formation a tradeoff between a biexciton and cavity-photon components in $|2p\rangle$ always arises and that this tradeoff affects the signal shape and peak intensity of the FWM of cavity bipolariton. A strong cavity-bipolariton signal was obtained when a cavity bipolariton formed by a superposition state of a biexciton and unbound two-cavity-polariton state was realized. Consequently careful control of cavity-QW parameters is necessary to form a cavity bipolariton. We also have analyzed the dynamics of the formation of biexciton and cavity polaritons by numerically solving the optical master equation in time domain in terms of the dependence on incident pulse duration σ. We have shown that an excitation tradeoff between a biexciton and photon components depends on σ and that there exists a specific pulse duration to achieve a strong FWM signal of the cavity bipolariton. In the dynamic formation process, efficient excitation of the cavity bipolariton could be realized when the immediate excitation to $|G;2\rangle$ by a subsequent input photon is suppressed, so that the LPB and UPB could grow enough. Simultaneous excitation of $|X;1\rangle$ and $|G;2\rangle$ therefore plays a key role in obtaining a strong FWM signal of cavity bipolariton.

In this analysis, we have restricted quantum-well excitons to a simplified one-dimensional model. This model enables us to analyze the cavity-bipolariton formation by providing a set of a biexciton state and unbound two-exciton states as a complete orthonormal system, though it needs modeling of exciton-exciton interaction and parametrization of the biexciton binding energy. For fully quantitative discussion of the realistic exciton system, however, the extension of our present approach to two-dimensional excitons is required. It would then be interesting to use microscopic theories of two-dimensional excitons[22,23] starting with electrons and holes, properly including spin degree of freedom, Coulomb interaction between excitons, and biexciton formation. Applications of such microscopic theories to a specific quantum-well microcavity system can be found, e.g., in Refs. 24 and 25, however the coupling between the photons and two-exciton states, especially biexciton-cavity coupling, is not discussed in them. The treatment based on the bipolariton framework in the present work would be desired and give useful perspectives on the practical requirement for the implementation of effective biexciton-cavity coupling. Note that in that case, it will take very long computation time to properly treat eigenstates of $2p$ states.

Finally, it would be interesting to consider the implications of our results for high-quality homogeneously broadened QW system. In this case, the generation and observation of cavity bipolaritons can be simplified.[26] In general, high-quality homogeneity of the sample enhances the excitonic coherence, and if the QW is wider, the exciton-photon coupling needs to be treated using the nonlocal theory[27] that properly includes spatial structure changes of exciton and photon wave functions. The extension of our approach to the nonlocal theory including biexciton states might thus be interesting.

In conclusion, effective biexciton-cavity coupling and delay excitation of biexciton appear to be essential for the realization of strong optical nonlinearity obtained from biexciton-cavity systems. The results presented in this work may thus help to identify some of the practical requirements for the implementation of nonlinear optical devices, especially entangled-photon generation based on the concept of cavity-biexciton (bipolariton) nonlinearity.[6,7]

ACKNOWLEDGMENTS

This work was supported by a Grant-in-Aid for Creative Scientific Research (No. 17GS1204) from the Japan Society for the Promotion of Science and KAKENHI (Grant-in-Aid for Scientific Research) on Priority Area "Strong Photons-Molecules Coupling Fields (No. 470)" from the Ministry of Education, Culture, Sports, Science, and Technology of Japan.

[1] M. A. Nielsen and I. L. Chuang, *Quantum Computation and Quantum Information* (Cambridge University Press, Cambridge, 2000).
[2] D. Bouwmeester, A. Zeilinger, and A. K. Ekert, *The Physics of Quantum Information: Quantum Cryptography, Quantum Teleportation, Quantum Computation* (Springer-Verlag, Berlin, 2000).
[3] K. Edamatsu, G. Oohata, R. Shimizu, and T. Itoh, Nature (London) **431**, 167 (2004).
[4] N. Akopian, N. H. Lindner, E. Poem, Y. Berlatzky, J. Avron, D. Gershoni, B. D. Gerardot, and P. M. Petroff, Phys. Rev. Lett. **96**, 130501 (2006).
[5] R. M. Stevenson, R. J. Young, P. Atkinson, K. Cooper, D. A. Ritchie, and A. J. Shields, Nature (London) **439**, 179 (2006).
[6] H. Ajiki and H. Ishihara, J. Phys. Soc. Jpn. **76**, 053401 (2007).
[7] H. Oka and H. Ishihara, Phys. Rev. Lett. **100**, 170505 (2008).
[8] T. Baars, G. Dasbach, M. Bayer, and A. Forchel, Phys. Rev. B **63**, 165311 (2001).
[9] P. Borri, W. Langbein, U. Woggon, J. R. Jensen, and J. M. Hvam, Phys. Rev. B **62**, R7763 (2000).
[10] G. C. La Rocca, F. Bassani, and V. M. Agranovich, J. Opt. Soc. Am. B **15**, 652 (1998).
[11] A. L. Ivanov, P. Borri, W. Langbein, and U. Woggon, Phys. Rev. B **69**, 075312 (2004).
[12] As long as we consider linearly polarized incident light, bound and unbound two-exciton states provided by this Hamiltonian include essentially the same physical properties of a complete system as those by the two-component Hamiltonian including the spin degree of freedom.
[13] H. Ishihara and K. Cho, Phys. Rev. B **48**, 7960 (1993).

[14] We choose t and Δ so that Δ_B can correspond to the experimental data. By comparing to the cavity dispersion, t is quite small and therefore the value of t hardly affects the results of this work.
[15] Th. Östreich, K. Schönhammer, and L. J. Sham, Phys. Rev. Lett. **74**, 4698 (1995).
[16] For biexciton excitation, another method, the incoherent regime by strong excitation, is also known. See, for instance, M. Saba, F. Quochi, C. Ciuti, U. Oesterle, J. L. Staehli, B. Deveaud, G. Bongiovanni, and A. Mura, Phys. Rev. Lett. **85**, 385 (2000). In this case, polariton states with higher photon numbers, such as $|3p\rangle = \alpha_{XXC}|XX;1\rangle + \alpha_{XCC}|X;2\rangle + \alpha_{CCC}|G;3\rangle$, are required.
[17] D. F. Walls and G. J. Milburn, *Quantum Optics* (Springer, Berlin, 1994).
[18] To be exact, owing to the difference in the excitation method between the present work and Ref. 8, our predicted value of $\hbar g_0^B$ might be slightly different from the actual value of the experiment in Ref. 8. However, this slight difference does not affect the following results of this work.
[19] We should also say that FWM signals due to the UPB-$2p$ transition can be found at ~ 1.412 eV on logarithmic scale, though they are much smaller than that due to the LPB.
[20] The peak intensity is also due to the linewidth of the LPB signal.
[21] The discontinuity of anticrossing points is due to the discrete model presented here. For the continuum limit of $N \to \infty$, the anticrossing points become continuous, as can be seen in the band structure in Figs. 2 and 4 (in fact, the level anticrossing due to the unbound two-exciton states occurs in the band structure).
[22] D. S. Chemla and J. Shah, Nature (London) **411**, 549 (2001).
[23] V. M. Axt and T. Kuhn, Rep. Prog. Phys. **67**, 433 (2004).
[24] S. Savasta, O. Di Stefano, and R. Girlanda, Phys. Rev. Lett. **90**, 096403 (2003).
[25] S. Schumacher, N. H. Kwong, and R. Binder, Phys. Rev. B **76**, 245324 (2007).
[26] P. Borri, W. Langbein, U. Woggon, J. R. Jensen, and J. M. Hvam, Phys. Status Solidi A **190**, 383 (2002).
[27] K. Cho, *Optical Response of Nanostructures: Microscopic Nonlocal Theory* (Springer, New York, 2003).